Supplementary Materials:

Classic reaction kinetics can explain complex patterns of antibiotic action

P. Abel zur Wiesch[1,2*], S. Abel[3], S. Gkotzis[4], P. Ocampo[5,6], J. Engelstädter[7], T. Hinkley[8], C. Magnus[9], M. K. Waldor[3], K. Udekwu[4], T. Cohen[1,2,10]

[1] Division of Global Health Equity, Brigham and Women's Hospital and Harvard Medical School, 641 Huntington Avenue, Boston, Massachusetts 02115, United States of America.

[2] Present address: Division of Epidemiology of Microbial Diseases, Yale School of Public Health, 60 College Street, New Haven, Connecticut 06510, United States of America.

[3] Division of Infectious Diseases, Brigham and Women`s Hospital and Harvard Medical School and HHMI, 181 Longwood Avenue, Boston, Massachusetts 02115, United States of America.

[4] Department of Neuroscience, Karolinska Institutet, Retzius väg 8, 17177 Stockholm, Sweden.

[5] Institute of Integrative Biology, ETH Zürich, Universitätsstrasse 16, 8092 Zürich, Switzerland.

[6] Department of Environmental Microbiology, EAWAG, Überlandstrasse 133, 8600 Dübendorf, Switzerland.

[7] School of Biological Sciences, The University of Queensland, Brisbane, QLD 4072, Australia.

[8] School of Chemistry, University of Glasgow, University Avenue, Glasgow, G12 8QQ, UK.

[9] Institute of Medical Virology, University of Zürich, Winterthurerstrasse 190, 8057 Zürich, Switzerland.

[10] Department of Epidemiology, Harvard School of Public Health, 677 Huntington Avenue, Boston 02115, MA, United States of America.

*Correspondence to: pzw@daad-alumni.de

Supplementary materials and methods.

Single cell time-lapse microscopy

The specific details of the microfluidic system used in this study have been described previously (*36*). Briefly, this device consists of 4000 growth channels arranged at right angles to a trench through which growth media is passaged. To prepare the inoculums for these experiments, overnight cultures of *E. coli* MG1655 were grown in LB at 37 °C, then the cultures were diluted 1:100 in pre-warmed LB and incubated with shaking at 37 °C for 2 h. Cells were then concentrated 400-fold and 10 μL of the resulting cell suspension was injected into the microfluidic system and incubated without media flow. The experiment was initiated when more than 80% of the growth channels were filled with cells via diffusion. A syringe pump was used to passage fresh LB supplemented with bovine serum albumin (BSA) and salmon sperm DNA through the device at a constant flow rate of 2 mL/h. BSA and salmon sperm DNA are blocking agents used to bind to the surface of the microfluidic device to prevent the formation of air bubbles and excessive adhesion of the cells to the channels. Images were acquired from different fields of view at 6 min intervals via an automated Olympus BX81 microscope equipped with a UPLFN100xO2PH/1.3 phase-contrast lens and an automated stage. Samples were held at 37°C with a Cube and Box incubation system (Life Imaging Services). After at least 4 h of growth in LB, the medium was switched to LB containing BSA, salmon sperm, and antibiotics. Cells were exposed to this regimen for at least 20 h before being switched back to fresh LB supplemented with BSA and salmon sperm DNA for up to 10 h. The resulting time-lapse images were analyzed with the MMJ plugin for ImageJ (available at http://projects.exeter.ac.uk/ein/mmj/doku.php) to acquire information on cell elongation and division rates during the experiment. Manual verification and annotation were performed for every experiment. A different analysis of two out

of the 5 datasets (12.5 mg/L tetracycline and 25 mg/L streptomycin) was published elsewhere (*36*).

Growth curves (turbidity-based)

For these experiments, $5x10^7$ cfu/ml (*E. coli* MG1655 in MHII medium and *V. cholerae* C6706 in LB medium) derived from exponentially growing bacterial cultures were used. A 1:2 dilution series was created and respective antibiotics were added. A range of antibiotic concentrations (Table S1) above and below MIC were chosen such that the highest did not clear all bacterial densities and the lowest suppressed at least the lowest density. The MIC was defined according to CLSI as no growth over 18 h with an initial density of $5x10^5$ cells/ml in 96-well plates as observed by turbidity measurements. Growth was recorded for 12 h by determining absorption at 600 nm in 10 min (*V. cholerae*) to 15 min (*E. coli*) intervals in a Bioscreen C plate reader using 10x10 honeycomb plates (Oy Growth Curves Ab Ltd) for *V. cholerae* and a Synergy Mx Monochromator-Based Multi-Mode Microplate Reader (BioTek) using 96 well plates (Sarstedt) for *E. coli*. All conditions were measured in biologically independent triplicates.

We verified a linear relationship between OD_{600} and cfu/ml over a range of 0.01 to 1 OD_{600}. All values below 0.01 OD_{600} were assumed to reflect noise. To quantify antibiotic efficacy, we used the total bacterial burden as measured by the average density over 12 h. To calculate the relative bacterial burden, the total bacterial burden at each antibiotic concentration was normalized to the bacterial burden in the positive control without antibiotic and the same initial bacterial density.

Quantification of inoculum effect

At a given antibiotic concentration, we found a linear relationship between the logarithm of relative bacterial burden and the logarithm of initial bacterial density. The slope of this relationship is a measure of antibiotic efficacy loss with increase of bacterial density ('inoculum effect'), and was determined by a linear regression of $\log_{10}$ relative bacterial burden vs. $\log_{10}$ initial density. To characterize the strength of the inoculum effect for each antibiotic, the mean of the slopes of these regressions over all employed antibiotic concentrations were used.

Growth curves (cfu-based)

Time kill experiments were performed as described previously (*59*). Briefly, a standardized inoculum of final concentration, C_f, ~$5x10^5$ cfu/ml was added to MHII containing or not the antibiotic in question in 12 well culture plates. The range of antibiotic concentrations used was 0.5, 1, 2, 4, 8, 12 and 16 times the reported MIC. All cultures were sampled at the initial time of inoculation and followed over 18 h. Sampling was performed in biologically independent triplicates. All samples were diluted appropriately and plated on LB plates. Colony forming units (cfu) were counted up to 3 days after incubation at 37 ^oC to account for slower growing cfu. Results for control and antibiotic treated cultures were plotted against time.

Minimum inhibitory concentration determination

Minimum inhibitory concentrations (MICs) were estimated by the broth microdilution protocol as recommended by Clinical and Laboratory Standards Institute (CLSI) guidelines (*16*). Cultures were incubated in 96-well plates, at 37˚C with vigorous shaking at 200 rpm and growth was

monitored on a Biotek plate-reader via absorbance values at OD_{600}. MIC was determined as a function of growth or non-growth, defined as $OD_{18h}–OD_{0h}<0.02$ absorbance units.

Modeling approach

1. General framework

The action of antibiotics is described as a multistep binding process to bacterial target molecules (Fig. 8). We assume that bacteria have a set number of target molecules that may vary between individual bacterial cells. We do not model binding to several different targets explicitly, rather we subsume target binding with single apparent association (and for reversible reactions dissociation) rates: $A+T \underset{k_r}{\overset{k_f}{\rightleftharpoons}} AT$. The intracellular antibiotic molecules A react with target molecules T with a rate k_f and form an antibiotic-target molecule complex. If the reaction is reversible, the complex dissociates with a rate k_r, leading to a dynamic equilibrium. If the reaction is irreversible, equilibrium is reached when the effective concentration of the antibiotic is less than the concentration of target molecules (i.e., all antibiotic molecules have reacted, but some target molecules are still free). We then assume that the growth rate declines (bacteriostatic antibiotics) and/or the death rate increases (bactericidal antibiotics) with the number of bound target molecules. The bactericidal and bacteriostatic action of tetracycline and streptomycin at a given concentration was determined by single cell microscopy. The number of target molecules as well as the kinetic parameters for the antibiotics used in the study is given in table S2. In table S3 below, we list the abbreviations for the variables and parameters in our model:

2. Detailed description of antibiotic action

2.1 Bacteriostatic action only (antibiotics only affect replication)

At sub-inhibitory antibiotic concentrations, we only observed slower growth, but no bacterial death as defined by lysis or failure to resume elongation or replication after the post-antibiotic phase (Fig. S1). For translation inhibiting antibiotics such as tetracycline, the bacterial replication rate depends linearly on the fraction of free ribosomes (*37*). We therefore assume that the growth rate r is proportional to $f_{free} = \frac{[T]}{[T]+[AT]}$ above a critical threshold f_c below which cells do not replicate at all:

$$r(f_{free}) = \begin{cases} 0 & f_{free} < f_c \\ \frac{1}{1-f_c} f_{free} - f_c & f_{free} > f_c \end{cases} \quad (1)$$

Here, we track bacterial cells B (scaled in density per liter) that may multiply to a carrying capacity K, the extracellular and intracellular concentration of antibiotics $[A_e]$ and $[A_i]$, and the intracellular concentration of drug-target complexes $[AT]$ and unspecifically bound antibiotic $[AU]$. When considering transmembrane diffusion, we must follow both extracellular concentration $[A_e]$ and intracellular concentration of antibiotics $[A_i]$; here the bacterial membrane has a permeability coefficient p. Here, the rates k_f and k_r describe the kinetic rates for specific binding, the rates $k_{u,f}$ and $k_{s,r}$ describe the rates for unspecific binding. For ribosomes, it was shown that the total amount of ribosomes increases linearly with cell volume, i.e. the intracellular concentration within a single cell between its "birth" and the split into two daughter cells remains constant (*42*) (this does not preclude variation in a bacterial population, e.g. resulting from unequal distribution of target molecules to daughter cells). We can therefore write the concentration of free target molecules as $[T] = \frac{BT_0 - AT}{BV_i n_A}$, with the intracellular volume V_i

per cell and the Avogadro-number n_A (Table S3). The growth of bacteria at sub-MIC concentrations of a translation inhibitor can then be described by the following set of differential equations:

$$\begin{aligned}
\frac{dB}{dt} &= r(T_0,[AT],f_c)B(1-\frac{B}{K}) \\
\frac{dA_e}{dt} &= -pB([A_e]-[A_i]) \\
\frac{dA_i}{dt} &= pB([A_e]-[A_i])-k_f[A_i][T]+k_r[AT]-k_{u,f}[A_i]B+k_{u,r}[AU] \\
\frac{dAT}{dt} &= k_f[A_i][T]-k_r[AT] \\
\frac{dAU}{dt} &= k_{u,f}[A_i]B-k_{u,r}[AU]
\end{aligned} \tag{2}$$

For cells growing in microfluidic chambers, we assume that the extracellular antibiotic concentration and bacterial population size are constant.

2.2 Bactericidal action only (antibiotics affect only bacterial killing)

At low concentrations of streptomycin (80% MIC), bacterial growth is not affected (Fig. S4), but at 2x MIC bacterial killing is so fast that few bacteria replicate before they lyse. In this case, we can neglect the effect of antibiotics on bacterial replication and only consider bacterial killing.

The kinetics of antibiotic-target reaction can be described by the single differential equation, which can be simplified when the intracellular antibiotic concentration $[A]$ is constant:

$$\frac{d[AT]}{dt} = k_f[A]([T_0]-[AT])-k_r[AT] \tag{3}$$

and solved as

$$[AT](t) = \frac{k_f[A][T_0](1-e^{-(k_r+k_f[A])t})}{k_r+k_f[A]} \tag{4}$$

Here, we define the MIC as the antibiotic concentration at which 99% of the cells have bound a sufficient number of antibiotic molecules in equilibrium to be inactivated (either growth suppression or killing). Thus, when the MIC as well as the standard deviation σ of the susceptibility in a bacterial population are known, we can infer the thresholds (as fraction of total target molecules) that have to be reached for bacterial killing. $t_{c,99}$ indicates the critical threshold for the 99. Percentile of the bacterial population and $t_{c,50}$ the threshold for the median of the population. $[A]_{MIC}$ is the antibiotic concentration at the MIC. Then,

$$t_{c,99} = \frac{k_f[A]_{MIC}}{k_f[A]_{MIC}+k_r} = t_{c,50} - 2.58\sigma \quad (5)$$

Due to the limited sample size for intracellular ribosomal content, we cannot reliably determine the 99th percentile and define t_c in this case as the number of bound targets in equilibrium at the MIC for the cell with the lowest ribosomal content (i.e. the one that will reach the required threshold latest and is least susceptible, because the intracellular concentration of target is lowest).

We assume that bacterial death depends on the number of free and occupied target molecules, as described by equations (3) and (4). There are several ways that antibiotic-target binding may lead to bacterial death (Fig. 8).

The target molecules might have a function essential for bacterial survival that is inhibited by antibiotic binding (Fig. 8). In this case, bacteria die once the number of free target molecules is below a given threshold. It is also conceivable that the target-antibiotic complex is toxic for the

cell, such that exceeding a threshold of bound target molecules results in death. Finally, death might be mediated by secondary metabolites such as mistranslated proteins. In this case, bacterial death occurs once a threshold of these secondary metabolites is exceeded.

In the case of the prodrug isoniazid (INH), target binding occurs after drug activation to the adduct INH-NAD (equivalent to A before) which depends on NAD content and oxygen saturation (Fig. 7). Here, we focus on INH binding to the enoyl reductase InhA, which is then present in its inactive form $InhA_i$. Assuming NAD and INH concentration as well as oxygen saturation remain constant, this is described by the following set of equations:

$$\frac{d[INH \cdot NAD]}{dt} = k_{NAD,O_2}[INH] - k_f[INH \cdot NAD][InhA] + k_r[InhA_i] \tag{6}$$

$$\frac{d[InhA_i]}{dt} = k_f[INH \cdot NAD][InhA] - k_r[InhA_i]$$

The corresponding equations were solved numerically and the time until a given threshold was reached recorded. Variance in cellular molecule content was implemented by randomly sampling at least 1000 times from a normal distribution for the respective parameter.

2.3 Bacteriostatic and bactericidal action

To incorporate both growth and death into our model, we classify living bacteria in compartments that depend on the number of bound target molecules x (B_x, Fig. 8), out of a total of n target molecules. For this model, we ignore differences between extracellular and intracellular antibiotic concentrations and only follow the total antibiotic concentration A.

Here, bacterial cells with n target molecules are equivalent to molecules with n independent binding sites. The association and dissociation of target and antibiotic molecules is described by the following system of differential equations:

$$\begin{aligned}
\frac{dB_0}{dt} &= -\frac{k_f}{n_A V_i} nAB_0 + k_r B_1 \\
\frac{dB_x}{dt} &= \frac{k_f}{n_A V_i}(n-x+1)AB_{x-1} - k_r x B_x - \frac{k_f}{n_A V_i}(n-x)AB_x + k_r(x+1)B_{x+1} \quad for\ 1 < x < n \\
\frac{dB_n}{dt} &= \frac{k_f}{n_A V_i} AB_{n-1} - k_r n B_n \\
\frac{dA}{dt} &= -\frac{k_f}{n_A V_i}\sum_{x=0}^{n-1}(n-x)AB_x + k_r \sum_{x=1}^{n} x B_x \qquad for\ 0 \le x \le n
\end{aligned} \tag{7}$$

For streptomycin and high concentrations of tetracycline (which is static below MIC), we observe bacterial lysis quickly after cessation of elongation. i.e. cell death, described by the parameter d. When cells lyse upon death, the compartments of dead cells are replaced by a pool of free target molecules T and free antibiotic-target complexes AT (Fig. S8A). Here, we assume that the total intracellular volume of the bacterial population is so much smaller than the volume of the surrounding medium (at the highest density of 10^9 bacteria/ml, the intracellular volume is ~ 0.1%) that lysis does not change the extracellular antibiotic concentration. The extracellular compartments are then described by:

$$\begin{aligned}
\frac{dA}{dt} &= -\frac{k_f}{n_A V_i}(A\ T + \sum_{x=0}^{n-1}(n-x)AB_x + k_r(AT + \sum_{x=1}^{n} x B_x) \\
\frac{dT}{dt} &= -\frac{k_f}{n_A V_i} A\ T + k_r AT + \sum_{x=0}^{n} d_x (n-x) B_x \\
\frac{dAT}{dt} &= \frac{k_f}{n_A V_i} A\ T - k_r AT + \sum_{x=0}^{n} d_x x B_x
\end{aligned} \tag{8}$$

Living bacteria replicate with a rate r_x depending on the number of bound target molecules. Replication ceases when the total bacterial population approaches the carrying capacity K. We

assume that the total number of target molecules T doubles at replication, such that each daughter cell has the same number as the mother cell. The distribution of x bound target molecules of the mother cell to its progeny is described by hypergeometric sampling of n molecules from x bound and $2n$-x unbound molecules. The total rate ρ_x with which replication creates new bacteria with x bound target molecules depends thus on the number of bacteria L_i with at least x bound target molecules, their specific replication rate r_i and the fraction of their daughter cells expected to inherit x antibiotic-target complexes $f_{i,x}$:

$$\rho_x = 2\sum_{i=x}^{n} f_{i,x} r_i B_i \frac{K - \sum_{j=0}^{n} B_j}{K} \tag{9}$$

Taken together, each compartment of living bacterial cells can thus be described as:

$$\frac{dB_x}{dt} = \frac{k_f}{n_A V_i}(n-x+1)AB_{x-1} - k_r x B_x - \frac{k_f}{n_A V_i}(n-x)AB_x + k_r(x+1)B_{x+1} + \rho_x - r_x B_x \frac{K - \sum_{j=0}^{n} B_j}{K} - d_x B_x \tag{10}$$

The colors indicate the terms for association and dissociation as in equation (7), while the terms in black describe the additional population dynamics, i.e. growth and death.

If the cells do not lyse upon death, we distinguish between living (B_x) and dead (D_x) bacteria (Fig. S8B). We assume that association and dissociation rates of the target-antibiotic complex are the same in both cell types (i.e., that the chemical kinetics are not affected by death while the cell membrane is still intact). This modeling approach gives exactly the same results as the one where cells are assumed to lyse upon death.

For the simulations presented in figure 5B, we assume that bacteria die when more than 5% of targets are bound, that ciprofloxacin does not suppress bacterial growth below that threshold, and that there is a 10% standard deviation in the number of targets per cell.

Model fitting

We fitted equation (2), (growth inhibition only) to single cell data (obtained as described above) of bacteria exposed to 6.25 and 12.5 µg/ml tetracycline by minimizing the sum of squares of both experiments (equal weights) with the function nlm() in the statistical software package R (version 3.0.2). We estimate the following free parameters: net diffusion into cytosol p=2x10^{-11} m/s, critical fraction of free ribosomes f_c=2.6%, and unspecific association rate $k_{u,f}$=50 s^{-1} and unspecific dissociation rate $k_{u,r}$=0.99 s^{-1}. Note that in the case of each of these estimates, we are describing several processes with a single composite parameter.

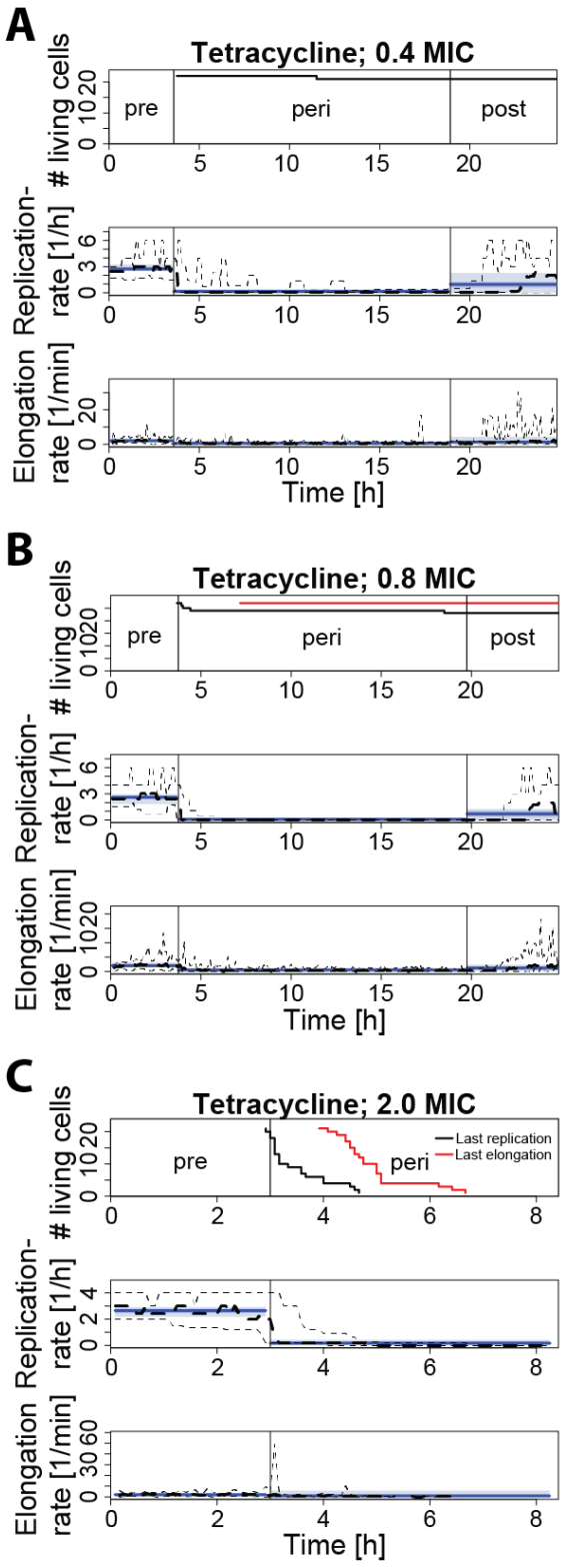

Fig. S1. Analysis of single cell time-lapse microscopy data *E. coli* MG1655 cells exposed to tetracycline. Cells were grown in a flow chamber supplied with medium without antibiotics for

4 h (pre-phase), exposed to antibiotic for 16h (peri-phase), followed by growth in medium that did not contain antibiotics for at least 4h (post-phase). Upper panel number (#) of living cells as measured by last replication (black line) or last elongation (red line); middle panel replication rate h^{-1}; lower panel elongation rate in pixel/min. Experimental mean in 5 min intervals (thick black line), experimental mean for entire pre-, peri- and post-exposure period (blue line), experimental minimum and maximum in 5 min intervals (thin, dotted black line), experimental minimum and maximum for entire pre-, peri- and post-exposure period (blue shaded area). (**A**) 22 bacteria were observed and exposed to 6.25 mg/L tetracycline (0.4x MIC) for 16 h. (**B**) 27 bacteria were observed and exposed to 12.5 mg/L tetracycline (0.8x MIC) for 16 h. This dataset is identical to that shown in Movie S1. (**C**) 21 bacteria were observed and exposed to 32 mg/L tetracycline (2x MIC) for 9 h.

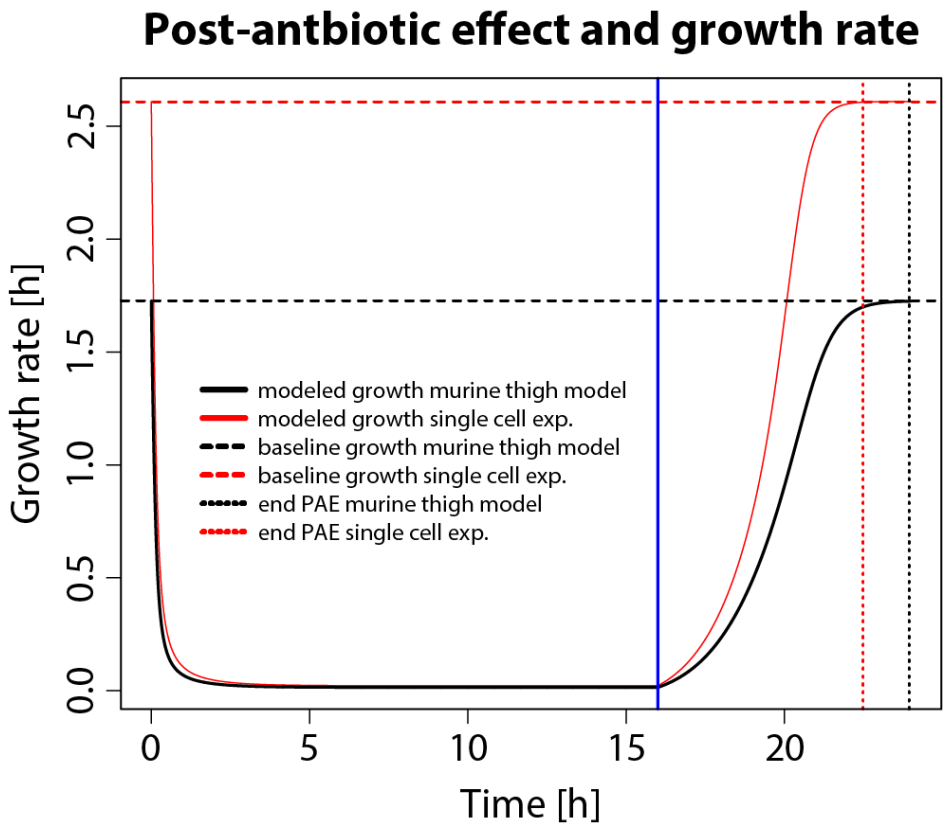

Fig. S2. Baseline growth rate affects length of post-antibiotic growth suppression. This figure compares the predicted length of post-antibiotic growth suppression between our single-cell experiment (compare to figure 1A, red) and a hypothetical bacterial population that is identical except that the growth rate is lower (as measured in vivo (Vogelman, JID 1988), black). We define the post-antibiotic effect as the time the growth rate reaches 99.9% of the baseline growth rate after antibiotic exposure. X-axis: time-line in hours, y-axis: growth rate per hour, blue vertical line: withdrawal of antibiotic, dotted horizontal line: baseline growth in absence of drug, vertical dotted line: end of post-antibiotic effect.

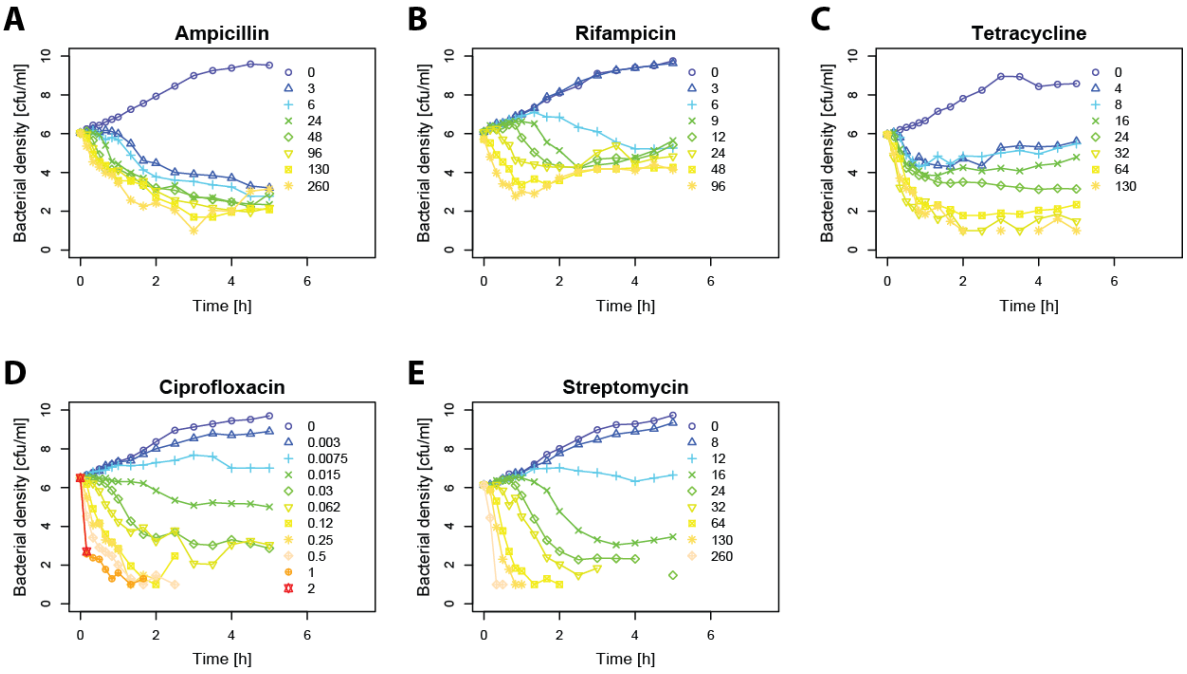

Fig. S3. Time-kill curves of *E. coli* CAB1 exposed to five different classes of antibiotics in various concentrations. To quantify persistence, the expected time to clearance was extrapolated from the initial kill rate between the onset of antibiotic action and 1 h after this time point. The onset of antibiotic action was defined as the first decrease in bacterial counts over two consecutive time-points to account for lag phases (e.g. streptomycin at intermediate concentrations). Persistence was quantified as the number of cfu/ml at the expected time to clearance. (**A**) ampicillin, 0 mg/L (blue) to 256 mg/L (orange), MIC= 3.4 ± 1.1, correlation persistence ~ concentration: not significant (n.s.); (**B**) rifampin, (blue) 0 mg/L to 96 mg/L (orange), MIC= 12.0 ± 1.9, correlation persistence ~ concentration: not significant (n.s.); (**C**) tetracycline, 0 mg/L (blue) to 128 mg/L (orange), MIC= 0.67 ± 0.68, correlation persistence ~ concentration: not significant (n.s.); (**D**) ciprofloxacin, 0 mg/L (blue) to 2 mg/L (red), MIC= 0.017 ± 0.005, correlation persistence ~ concentration: adjusted R^2=0.7, p=0.011; (**E**) streptomycin, 0 mg/L (blue) to 256 mg/L (orange), MIC= 18.5 ± 3.3, correlation persistence ~ concentration: adjusted R^2= 0.78, p=0.012. Raw data provided by Regoes et al. (*41*).

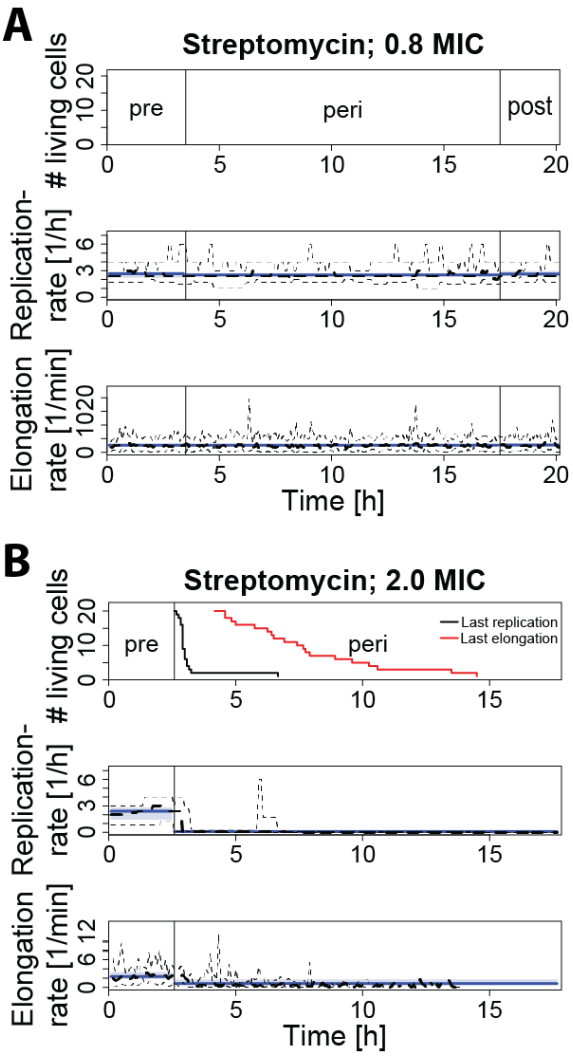

Fig. S4. Analysis of single cell time-lapse microscopy data for *E. coli* MG1655 cells exposed to streptomycin. Cells were grown in a flow chamber supplied with medium without antibiotics for 4 h (pre-phase), exposed to antibiotic for 16h (peri-phase), followed by growth in medium that did not contain antibiotics for at least 4h (post-phase). Upper panel number (#) of living cells as measured by last replication (black line) or last elongation (red line); middle panel replication rate h^{-1}; lower panel elongation rate in pixel/min. Experimental mean in 5 min intervals (thick black line), experimental mean for entire pre-, peri- and post-exposure period (blue line), experimental minimum and maximum in 5 min intervals (thin, dotted black line), experimental minimum and maximum for entire pre-, peri- and post-exposure period (blue shaded area). (**A**)

20 bacteria were observed and exposed to 10 mg/L streptomycin (0.8x MIC) for 16 h. (**B**) 21 bacteria were observed and exposed to 25 mg/L streptomycin (2x MIC) for 9 h. This dataset is identical to that shown in Movie S2.

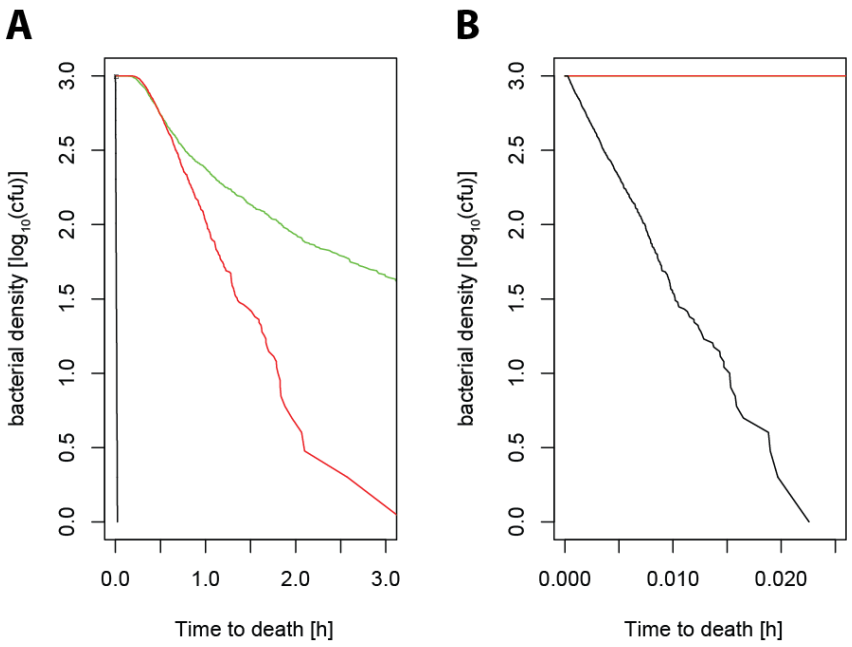

Fig. S5. Simulated time-kill curves under different assumptions. (**A**) Binding data for streptomycin were used (Table S2, methods), we assume 100 target molecules and the time to kill was simulated by implementing the reaction $A + T \underset{k_r}{\overset{k_f}{\rightleftharpoons}} AT$ in a Gillespie-Algorithm (10^3 replications). We assume that the target is essential, i.e. count the time until threshold of bound target molecules is exceeded. The black line indicates a threshold of 1, i.e. the cell dies when one target molecule is bound. The red line shows a simulated time-kill curve when the threshold is 50, i.e. the cell dies when 50% of the target molecules are bound. For the green line, we also assumed a mean threshold of 50% for killing, but allowed this threshold to vary by 15%. (B) Same as in (A) with different timeframe.

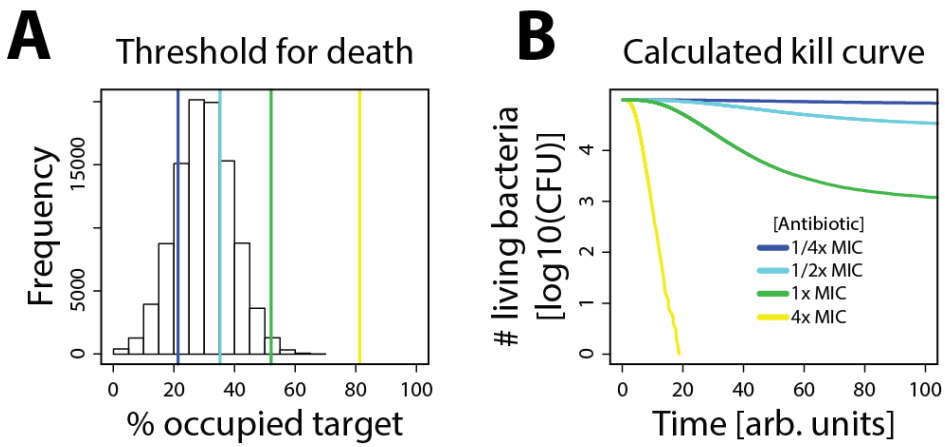

Fig. S6. Distribution of drug susceptibility and expected time-kill curve. This graph compares time-kill curves resulting from a normal distribution of susceptibility (A,B) and a bimodal distribution of susceptibility (Fig. 3 D,E) The MIC was calculated as the drug concentration that achieves binding of 99% of the cells at equilibrium (equation 5). The main "peak" of the bimodal distribution in Fig. 3 D corresponds to the normal distribution in A).

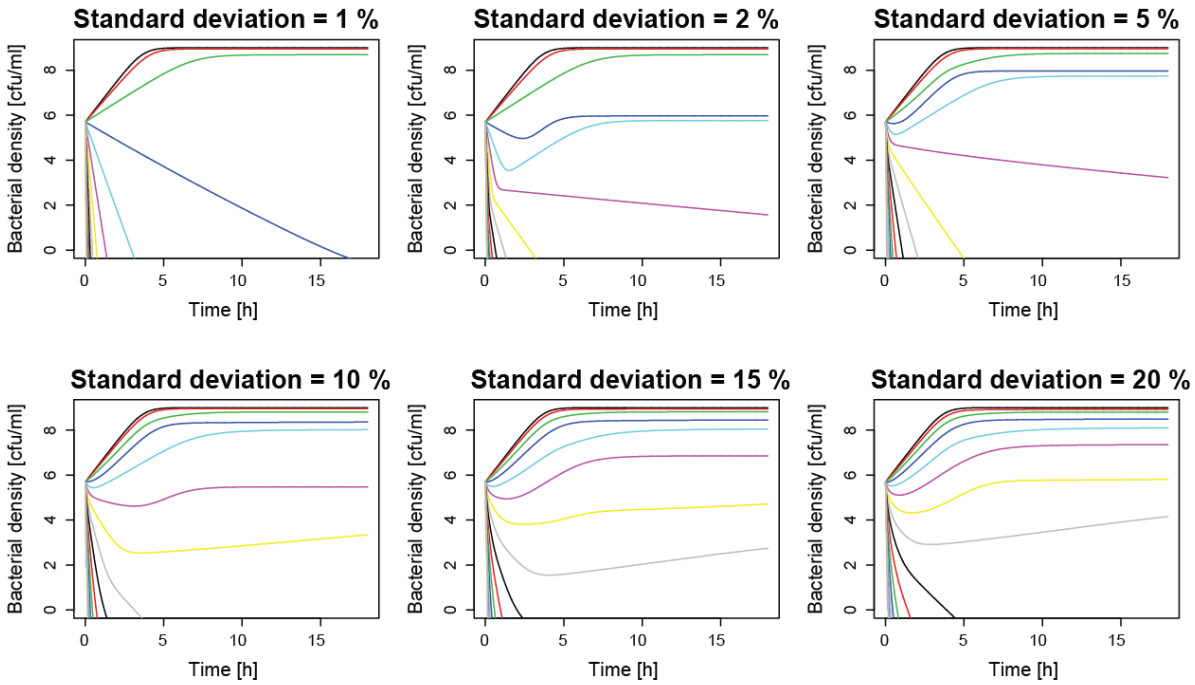

Fig. S7. Effect of variance in target molecule content. Simulated time-kill curves for bacteria exposed to different ciprofloxacin concentrations with same set of parameters as in figure 5B, but with increasing variance in the threshold of bound target molecules required for bacterial death. The concentration of ciprofloxacin increases from 0 µg/L (uppermost black line) to 80 µg/L in 5 µg/L increments.

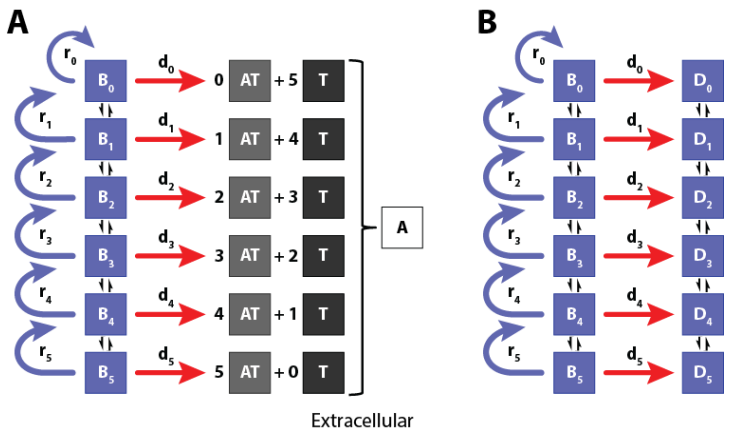

Fig. S8. Overview of kill mechanisms, chemical reactions, and compartmental models used in this study. The extracellular compartments are described as follows: *T* refers to free target molecules, *A* to the free antibiotic molecules, and *AT* to the antibiotic-target complex. *B* denotes living cells, *D* dead but intact cells, *r* the growth rate, and *d* the death rate. The subscripts refer to the number of bound target molecules in the different compartments. (**A**) Compartmental model of bacterial population with lysis. In this model, we assume that bacteria lyse when dying. (**B**) Compartmental model of bacterial population without lysis. In this model, we assume that the bacterial cell wall remains intact after death.

OD_{600} after 18 h	**S1**	**S2**	**S3**	**S4**	**S5**	**S6**	**S7**	**S8**	**S9**	**S10**	**pre-exposure**
8 µg/L	0.002	0.002	0.001	0.005	0.003	0.004	0.003	0.002	0.003	0.003	0.005
4 µg/L	0.613	0.603	0.583	0.596	0.568	0.608	0.560	0.565	0.709	0.655	0.554

Table S1. Ciprofloxacin persisting *E. coli* have not acquired higher resistance to the antibiotic. To test if *E. coli* populations that survived 18 h exposure to 8 µg/L ciprofloxacin have acquired inheritable resistance to the antibiotic, samples from the population were taken and individual clones were isolated. These bacteria (S1-S10) and their naïve (pre-exposure) parental control strain were re-exposed to media either containing 4 µg/L (1/2x MIC of the parental control strain) and 8 µg/L (1x MIC of the parental control strain) ciprofloxacin. The table shows turbidity measurements (OD_{600}) of *E. coli* after 18 h incubation. The suppression of growth at 8 µg/L in all samples indicates that exposure to ciprofloxacin did not lead to acquisition of resistance.

Antibiotic / organism	*E. coli* (MG1655)	MIC	*V. cholerae* (C6706)	MIC
Ampicillin [mg/L]	256; 128; 96; 64; 48; 32; 16	8	800; 400; 200; 100; 50; 25; 12.5; 6.25; 3.13	200
Ciprofloxacin [μg/L]	-	-	5; 3.75; 2.81; 2.11; 1.58; 1.19; 0.89; 0.67; 0.5	5
Gentamycin [mg/L]	8; 4; 2; 1; 0.5; 0.25; 0.125	1	30; 22.5; 16.9; 12.7; 9.5; 7.1; 5.3; 4; 3	16.9
Nalidixic acid [mg/L]	30; 15; 7.5; 3.8; 1.9; 0.9; 0.5; 0.2; 0.1	7.5	-	-
Penicillin [mg/L]	-	-	800; 400; 200; 100; 50; 25; 12.5; 6.25; 3.13	25
Rifampicin [mg/L]	-	-	0.4; 0.3; 0.23; 0.17; 0.13; 0.094; 0.071; 0.053; 0.04	0.13
Streptomycin [mg/L]	24; 16; 12; 8; 6; 4; 2	6	-	-
Tetracycline [mg/L]	16; 12; 8; 6; 4; 2; 1	2	0.5; 0.38; 0.28; 0.21; 0.16; 0.12; 0.09; 0.07; 0.05	0.21

Table S2. Antibiotic concentrations used for experiments.

Target	Antibiotic	Parameter	Value
Ribosome	-	Copy #/cell[a)]	55000 [~10^4-10^5]
	Tetracycline	K_D[b)]	1.1-3.2x10^{-6} M
		k_f[c)]	3x10^5 $M^{-1}s^{-1}$
		$k_r=K_D \times k_f$[d)]	0.33-0.96 s^{-1}
	Gentamicin	K_d[e)]	6x10^{-7} M
		k_r[d)]	-
		k_f[d)]	-
	Streptomycin	K_D[f)]	1.2-2.7x10^{-7} M
		k_f[d)]	-
		k_r[d)]	-
Penicillin binding proteins	-	Copy #/cell[g)]	~ 2500±120
	Ampicillin[h)]	Irreversible	
		k_f[i)]	130±1 $M^{-1}s^{-1}$
		Deacetylation rate (k_a)[i)]	1x10^{-4} s^{-1}
	Benzylpenicillin[h)]	Irreversible	
		k_f[i)]	590±100 M^{-1} s^{-1}
		Deacetylation rate (ka)[i)]	6x10^{-5} s^{-1}
Gyrase/Topoisomerase IV & DNA	-	Copy #/cell[j)]	Gyrase: 50-100 functional tetramers
	Ciprofloxacin	K_D[k)]	~10^{-5}
		k_f[d)]	
		k_r[d)]	
RNA Polymerase		Copy #/cell	1500 slow, 11400 fast growth[l)]
	Rifampicin	K_d[m)]	10^{-9} M
		k_f[m)]	1.2x10^6 $M^{-1}s^{-1}$
		k_r[m)]	1.2x10^{-3} s^{-1}
enoyl acyl carrier protein reductase (inhA)	Isoniazid (all values for *M. tuberculosis*)	rate of drug activation (INH+NAD->INH-NAD)[n)]	1.8x10^{-6} s^{-1}
		K_D[o)]	10^{-7} M
		$k_f=k_r/K_d$[p)]	2.8x10^3 $M^{-1}s^{-1}$
		k_r[p)]	2.8x10^{-4} s^{-1}

Table S3. Kinetic parameters for different antibiotics. a) (*42*, *64*, *65*); b) Tetracycline binds reversibly to six sites in the ribosome. However, one primary target site binds most strongly and seems to be mainly responsible for inhibition of translation (*66–68*). For 70S particles, the equilibrium constant K_D for this site is in the range of 1.1-3.2 µM, depending on Mg^{2+} concentration. (*66*); c) The apparent association rate of tetracycline to the ribosome was estimated to be ~3x10^5 M^{-1} s^{-1} (*69*). For simplicity, we assume here that the primary binding site alone is responsible for antimicrobial activity and its association rate is equal the apparent association rate. d) To our knowledge, these rates have not been determined. e) Ribosomes have a single non-cooperative site and 5 weaker cooperative binding sites for gentamicin. Here, we ignore weaker binding sites. (*70*); f) (*71–73*); g) (*47*, *74*); h) Binding rates for Pbp1a are given. In

Staphylococcus aureus, the binding rates do not differ substantially between different classes of Pbps, and we assume that the binding rates are equal for all Pbps (*46*). i) (*75*); j) Data for *E. coli* unknown; values are given for *Mycoplasma pneumoniae* and *Leptospira interrogans.* (*76*, *77*); k) (*74*, *75*); l) Doubling times 100 and 24 min, respectively. (*65*); m) (*78*); n) Calculated for a cellular NAD content of *E. coli* (*79*). For the drug-activating enzyme, KatG, the number of molecules per cell is unknown. Instead, we chose the average number of proteins in *E. coli* cells from (*80*). (*63*); o) (*81*); p) (*82*).

Variables		Parameters	
A_e	extracellular antibiotic	k_f	rate of forward reaction
A_i	intracellular antibiotic	k_r	rate of backward reaction
T	free target	p	permeability coefficient bacterial membrane
AT	bound target	f_c	Critical threshold free ribosomes for replication
AU	unspecifically bound antbiotic	n_A	Avogadro constant (6.02×10^{23})
		V_i	intracellular volume ($\sim 10^{-15}$L/ bacterial cell)
		K	Carrying capacity (10^9 bacteria/ml = 10^{12}/L)
		$k_{u,f}$	rate of unspecific forward reaction
		$k_{u,r}$	rate of unspecific backward reaction
		k_{tox}	rate of toxic metabolite formation
B_x	total bacterial cells with *x* bound target molecules	d_x	death rate of cells with *x* bound target molecules
L_x	living bacterial cells with *x* bound target molecules	r_x	growth rate of cells with *x* bound target molecules
D_x	dead bacterial cells with *x* bound target molecules	$f_{i,x}$	fraction of cells with *i* bound target molecules producing progeny with *x* bound target molecules

Table S4. Explanation of variables and parameters.

Movie S1. Single cell microscopy data for *E. coli* MG1655 cells exposed to 12.5 mg/L tetracycline (0.8x MIC). Cells were grown in a flow chamber supplied with medium without antibiotics for 4 h (pre-phase), exposed to antibiotic for 16 h (peri-phase), followed by growth in medium that did not contain antibiotics (post-phase). The dataset is identical to that shown in figure S1A.

Movie S2. Single cell microscopy data for *E. coli* MG1655 cells exposed to 25 mg/L streptomycin (2x MIC). Cells were grown in a flow chamber supplied with medium without antibiotics for 4 h (pre-phase), exposed to antibiotic for 9 h (peri-phase). The experiment was terminated early because no cell survived (i.e. all cells lysed). The dataset is identical to that shown in figure S4B.